Novel Family of Gelators of Organic Fluids and the Structure of Their Gels[1]

Yih-chyuan Lin,[†] Bechara Kachar,[‡] and Richard G. Weiss*,[†]

Contribution from the Department of Chemistry, Georgetown University, Washington, D.C. 20057, and Laboratory of Neuro-otolaryngology, NIDCD, National Institutes of Health, Bethesda, Maryland 20205. *Received January 17, 1989*

Abstract: The macroscopic and microscopic properties of a new family of thermally reversible gelators (ALS) of organic fluids and their gels have been investigated by a variety of techniques. Each ALS contains a 2-substituted anthracenyl-type group coupled directly or indirectly to C3 of a steroidal group. Only weak intermolecular interactions (dipolar and van der Waals forces) need hold the gelator networks in place. In spite of this, a gel of 2% cholesteryl 4-(2-anthryloxy)butanoate (CAB) in 4-heptanol can be retained in a sealed vessel at room temperature for several months. Experiments with a variety of organic fluids demonstrate that specific gelator–solvent interactions are not necessary for the gels to form. Thus, *n*-alkanes from heptane to hexadecane afford the same gelation temperature (T_g) with CAB. Molecular shape of the fluid is an important factor in T_g since methylcyclohexane is gelled by CAB at a lower temperature than are the *n*-alkanes, and 4-heptanol is gelled at a higher temperature. The kinetics of gel formation and the T_g have been followed by changes in intensities of absorption, fluorescence, and circular dichroism spectra. The intermolecular packing arrangement among neighboring CAB gelator molecules has been probed by using the above spectral techniques in addition to X-ray diffraction and ^{1}H NMR studies. They indicate a stacked, helical arrangement for CAB molecules with the anthracenyl groups overlapping partially. Optical and electron microscopies have allowed the gelator structure in CAB/1-octanol and CAB/dodecane gels to be elucidated: they consist of molecular domains (several micrometers in diameter) of fibrous bundles; the fibers have rectangular cross sections of 20.9 nm × 10.4 nm (dodecane gel) and 25.3 nm × 8.2 nm (1-octanol gel). Additionally, the fibers of the CAB/1-octanol gel are helically twisted. These results are compared with information from other gel systems in which the gelator forms intertwined fibers.

Previously, we reported that very small quantities of cholesteryl 4-(2-anthryloxy)butanoate (CAB) can gel reversibly with a wide variety of organic solvents.[2] Statistically, each CAB can gel more than 500 molecules of selected fluid components. We have also noted that the photodimer distribution from irradiation of the neat cholesteric mesophase of CAB is nonstereoselective, indicative of random parallel and antiparallel packing between neighboring molecules.[3]

In fact, CAB is only one member of a new family of gelators (ALS) of organic fluids whose aggregate structures rely upon weak attractive intermolecular interactions (dipolar and van der Waals forces). Except for the recently reported gelation of *n*-alkanes by relatively large concentrations of partially fluorinated *n*-alkanes[4] (that must also rely upon dipolar and van der Waals attractive forces), the behavior of the ALS appears to be unique. All of the effective ALS are relatively small molecules (MW < 700) that contain only carbon, hydrogen, and oxygen. Their basic components are an aromatic (A) and a steroidal group (S) with connecting atoms (L). In this paper, we report on the structural limitations of the ALS that act as gelators and provide more details on the properties of the gels that CAB forms, including the micromorphology of the gelator networks.

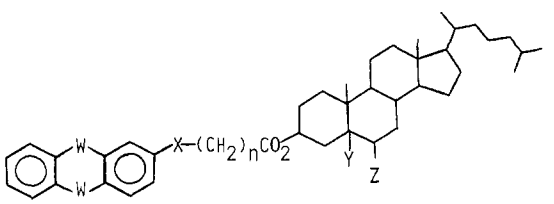

ALS GELATORS

	W	X	Y	Z	N
CA-2	CH	NO ATOM	NO ATOM	H	0
CAQ	CO	NO ATOM	NO ATOM	H	0
CAB	CH	O	NO ATOM	H	3
KAB	CH	O	NO ATOM	O	3
CAP	CH	O	NO ATOM	H	4
CHAQ	CO	NO ATOM	H	2H	0

[†]Georgetown University.
[‡]National Institutes of Health.

Two operational criteria have been expressed by Flory[5] to identify gel phases: they must appear solidlike with low elasticity and, above a finite yield stress, be deformed mechanically; they must possess a continuous structure throughout their microscopic dimensions (i.e., a degree of structural permanency that is continuously manifested). A practical consequence of these is that the gelator molecules must interact to provide a colloidal network for encapsulation of microregions of the fluid component. These interactions typically are stronger than dipolar or van der Waals forces (e.g., covalent or hydrogen bonds[5]).

Results and Discussion

Structural Limitations of ALS Molecules that Act as Gelators. Covalent linkage between the A and S groups is necessary (but not sufficient) for an ALS to act as a gelator. Thus, a solution comprised of 4.3/4.7/91 (w/w/w) anthracene/cholesteryl myristate/dodecane formed no gel above ca. 5 °C. Warm dodecane solutions of 2.8% of 2-dodecyloxyanthracene, 1.4% of ethyl 4-(2-anthryloxy)butanoate, or 1.8% of 1,2-di(4-(2-anthryloxy)butanoyloxy)ethane (**1**) led only to precipitates when cooled. A summary of these experiments is presented in Table I.

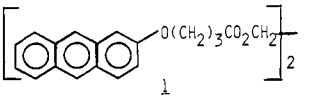

1

Some molecules that consist of one or two parts of an ALS have been found to be gelators under rather limited conditions. Desvergne and Bouas-Laurent[6] observed recently that methanol is gelled efficiently by an AL_2 molecule; under the same conditions, neither CAB nor 2-dodecyloxyanthracene gels either methanol or ethanol. The presence of two chains and their orientation must imbue the AL_2 with gelling properties that are quite different from those of the monoethers. Also, a group of steroidal molecules capable of both donating and accepting hydrogen bonds (**2**, an

(1) Part 37 in our series Liquid-Crystalline Solvents as Mechanistic Probes. For Part 36, see: Sonnenschein, M. F.; Weiss, R. G. *Photochem. Photobiol.*, submitted.
(2) Lin, Y.-C.; Weiss, R. G. *Macromolecules* **1987**, *20*, 414.
(3) Lin, Y.-C.; Weiss, R. G. *Liq. Cryst.* **1989**, *4*, 367.
(4) (a) Twieg, R. J.; Russell, T. P.; Siemens, R.; Rabolt, J. R. *Macromolecules* **1985**, *18*, 361. (b) Mahler, W., private communication.
(5) Flory, P. J. *Discuss. Faraday Soc.* **1974**, *57*, 7.
(6) Bouas-Laurent, H.; Desvergne, J.-P., private communication.

0002-7863/89/1511-5542$01.50/0

Table I. Nonsteroidal Compounds Containing Anthracenyl Groups Tested as Gelators

compound	% of gelator[a]/solvent	cooling method	phase formation[b]
anthracene	1.3–10/dodecane	*c, d*	soln
	8.2/1-octanol	*c, d*	soln
anthracene + cholesteryl myristate (CM)	4.28 (anthracene) + 4.67 (CM)/dodecane	*c, d*	soln
		c, d	
2-methoxyanthracene	2.3/dodecane	*c*	ppt
2-(1-dodecyloxy)anthracene	2.8/hexadecane	*c*	ppt
anthracene-9-carboxylic acid	1.5/dodecane	*c*	ppt
4-(2-anthryloxy)butanoic acid	1.6/dodecane	*c*	ppt
ethyl 4-(2-anthryloxy)butanoate	1.43/hexadecane	*c*	ppt
1,2-bis(4-(2-anthryloxy)butanoyl)ethane	1.8/doecane	*c*	ppt

[a] By weight. [b] ppt = precipitate; soln = solution. [c] Cooled to ambient temperatures in the air. [d] Cooled under cold running water (ca. 5 °C).

Table II. Non-Cholesteryl Steroids Containing Anthracenyl or Anthracenyl-Like Groups Tested as Gelators

compound	% of gelator[a]/solvent	cooling method	phase formation[b]
estrone 4-(2-anthryloxy)butanoate	1.41/dodecane	*c*	sol–ppt
	1.41/4-heptanol	*c*	ppt
	1.30/CCl_4	*c, d, e*	sol–ppt
pregnenolonyl 4-(2-anthryloxy)butanoate	1.89; 1.21/dodecane	*c*	ppt
	1.67/4-heptanol	*c*	ppt
	1.50/CCl_4	*c, d, e*	ppt
6-ketochlestanyl 4-(2-anthryloxy)butanoate (KAB)	1.13/dodecane	*c*	gel
	1.21; 0.89/1-octanol	*c*	gel
	1.20/CCl_4	*d, e*	sol
β-estradiol 3-benzoate 17-[4-(2-anthryloxy)butanoate]	1.30; 2.07/dodecane	*c*	sol–ppt
	1.23/1-octanol	*c*	ppt
17,21-dihydroxy-4-pregnene-3,11,20-trione-21-(4-(2-anthryloxy)butanoate)	1.42/dodecane	*c*	ppt
	1.05/1-octanol	*c, d*	soln
cholestanyl anthraquinone-2-carboxylate (CHAQ)	1.53/dodecane	*d*	gel
	2.91/4-heptanol	*c*	gel

[a] By weight. [b] ppt = precipitate; ppt–sol = precipitate and sol; soln = solution. [c] Cooled to ambient temperatures in the air. [d] Cooled under cold running water (ca. 5 °C). [e] Cooled in the freezing compartment of a refrigerator (<–10 °C).

S molecule) has been found by Terech and co-workers[7] to form very stable gels with cyclohexane, a fluid that is gelled by CAB only with great difficulty.

There are several common characteristics of the gel-effecting ALS molecules that we have synthesized: (1) they are capable of adopting rodlike shapes in their extended conformations; (2) they contain at least three fused aromatic rings; (3) they retain the C_8H_{17} alkyl chain at C17 of the steroid. However, several molecules that have all of these features still fail to act as gelators.

Steroidal Variations in ALS. Several esters of 4-(2-anthryloxy)butanoic acid in which the steroidal group lacks a C_8H_{17} chain at C17 were synthesized and tested as gelators. None of them, in combination with a variety of fluid components, produced a phase that could be identified visually as a gel (see Table II). Even solutions of β-estradiol 3-benzoate 17-[(4-(2-anthryloxy)-butanoate], an ALS somewhat like CAB but with the AL part attached to the D ring of the steroid, failed to form gels. The limitations on the length and branching of C17 steroidal chains in ALS that form gels have not been explored. Some modifications of cholesterol can lead to effective ALS gelators as witnessed by the 6-ketocholestanyl ester of 4-(2-anthryloxy)butanoate (KAB) and the cholestanyl ester of anthraquinone-2-carboxylate (CHAQ) that acted as gelators.

Aromatic Variations in ALS. Although cholesteryl anthracene-2-carboxylate (CA-2) is a gelator of dodecane, its 9 isomer (CA-9) is not. We have not synthesized (or tested) the 1 isomer (CA-1).[8]

Aromatic groups other than 2-substituted anthracenes can lead to ALS gelators. Dodecane and 4-heptanol were both gelled by cholesteryl anthraquinone-2-carboxylate (CAQ). However, cholesteric esters of smaller aromatic groups such as 4-phenylbenzoic acid and 2-naphthoic acid, although somewhat rodlike in shape, failed to gel any of the fluids tested (see Table III). Both the steric (shape-related) and electronic properties of an aromatic group must be germane to a molecule's gelating abilities since cholesteryl 4-(1-pyrenyl)butanoate, containing four nonlinearly fused aromatic rings, did not gel dodecane.

Linking Group Variations in ALS. The length of the linking group in 2-anthracenyl–cholesteric (ALS) molecules was investigated somewhat. As mentioned previously, CA-2 and CAB are effective gelators. The longer homologue of CAB, cholesteryl 5-(2-anthryloxy)pentanoate (CAP) also is effective. However, the shorter homologue, cholesteryl (2-anthryloxy)ethanoate (**3**) is not. We conjecture that the preferred conformer of the shorter ethanoate linking chain may project the anthracenyl and cholesteryl groups at an angle that destroys the molecule's ability to adopt a rodlike shape.[9]

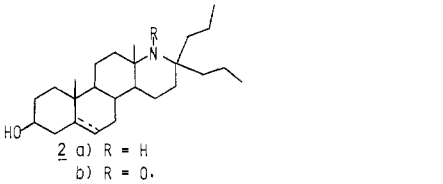

2 a) R = H
b) R = O.
(both with and without 5,6 double bond)

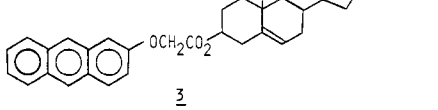

3

Fluids Gelled by CAB and Related ALS. Table IV provides a qualitative summary of the single-component fluids that were gelled by ca. 0.8–1.0% CAB. In each experiment, solid CAB and fluid were placed in a closed tube and heated until the solid dissolved or the liquid boiled without formation of a solution. Gelation was considered successful if the cooled solution formed

(7) (a) Wade, R. H.; Terech. P.; Hewat, E. A.; Ramasseul, R.; Volino, F. *J. Colloid Interface Sci.* **1986**, *114*, 442. (b) Terech, P.; Volino, F.; Ramasseul, R. *J. Phys. (Paris)* **1985**, *46*, 895. (c) Terech, P. *Mol. Cryst. Liq. Cryst.* **1989**, *166*, 29. See also: Zasadzinski, J. A. *J. Colloid Interface Sci.* **1988**, *122*, 288. Wade, R. H.; Terech, P. *Ibid.* **1988**, *122*, 291.

(8) If a rodlike shape is one requirement for an ALS to be a gelator of organic fluids, CA-1 will be less effective than CA-2.

(9) Attempts to synthesize cholesteryl 3-(2-anthryloxy)propanoate by two different approaches were unsuccessful.

Table III. Simple Cholesteric Compounds Tested Unsuccessfully as Gelators

compound	% of gelator[a]/solvent	cooling method	phase formation[b]
cholesterol hemisuccinate morpholine salt	1.3/dodecane	*c*	ppt-sol
	4.1/1-octanol	*c*, *d*	soln
	5.6/CCl_4	*c*, *d*, *e*	soln
cholesteryl aniline	1.1/dodecane	*c*, *d*, *e*	ppt
	1.1/1-octanol	*d*, *e*	soln
	2.9/CCl_4	*d*, *e*	soln
cholesteryl 4-biphenylcarboxylate	1.6/dodecane	*c*	soln
	4-5/dodecane	*c*	ppt
	1.7/1-octanol	*c*	soln
	1.6/CCl_4	*d*, *e*	soln
cholesteryl chloride	1-15/dodecane	*c*	soln
	1-13/1-octanol	*d*, *e*	soln
cholesteryl cinnamate	1-9/dodecane	*c*, *d*, *e*	soln
	1-14/1-octanol	*c*, *d*, *e*	soln
	3.6/CCl_4	*c*, *d*, *e*	soln
	1.8/2-octanone	*c*, *d*, *e*	soln
cholesteryl 9-fluorenone-2-carboxylate	1.4/dodecane	*c*	ppt
	1.2/4-heptanol	*c*	ppt
	1.1/CCl_4	*d*	ppt
cholesteryl 9-fluorenone-4-carboxylate	1.8/dodecane	*c*	ppt
	1.5/4-heptanol	*c*	ppt
	1.4/CCl_4	*d*, *e*	soln
cholesteryl hydrocinnamate	1-50/dodecane	*c*	soln
	1-50/4-heptanol	*c*, *d*, *e*	soln
	2.1/CCl_4	*c*, *d*, *e*	soln
cholesteryl myristate	5.1/hexadecane	*c*, *d*	soln
	12/hexadecane	*c*, *d*	soln
cholesteryl 3-naphthoate	1.8/dodecane	*c*	ppt
	1-1.5/1-octanol	*c*	ppt-sol
	1.9/CCl_4	*d*, *e*	soln
cholesteryl 2-(2-naphthoxy)acetate	1.7/dodecane	*c*	ppt (crystal)
	1.5/4-heptanol	*c*, *d*, *e*	sol
	1.4/1-octanol	*c*, *d*, *e*	sol
cholesteryl nonanoate	4.8/hexadecane	*c*, *d*	soln
	41.4/hexadecane	*c*, *d*	soln
cholesteryl oleate	1-70/dodecane	*c*, *d*	soln
	1-50/4-heptanol	*c*, *d*	soln
cholesteryl phenylacetate	1.4/dodecane	*c*	sol
	1.5/1-octanol	*c*, *d*	soln
	2.1/CCl_4	*c*, *d*, *e*	soln
cholesteryl 1-pyrenylbutanoate	1.5/dodecane	*c*, *d*	soln
	1.7/1-octanol	*c*, *d*	soln
	1.3/CCl_4	*c*, *d*, *e*	soln
dicholesteryl sebacate	1.7/dodecane	*c*	sol
	1.6/1-octanol	*c*	sol
	2.1/CCl_4	*c*, *d*, *e*	soln

[a] By weight. [b] ppt = precipitate; ppt-sol = precipitate and soil; soln = solution. [c] Cooled to ambient temperatures in the air. [d] Cooled under cold running water (ca. 5 °C). [e] Cooled in the freezing compartment of a refrigerator (<−10 °C).

a nearly transparent mass that could be inverted without apparent flow. The point at which a cooling "isotropic" solution containing 0.8% CAB (w/w) first exhibited a large increase in fluorescence intensity was taken as the gelation temperature, T_g (vide infra).[2] The T_g are independent of *n*-alkane length from heptane to hexadecane, indicating that fluid–gelator interactions need not be strong. However, the dependence of gelation on fluid molecular shape (and, therefore, specific gelator–fluid interactions) could be demonstrated with cyclohexane and methylcyclohexane: both formed very unstable gels with lower T_g than that of the *n*-alkanes (Figure 1).

The aliphatic and aromatic amines listed in Table IV required quick cooling to subambient temperatures to attain gelation. Nonanoic acid was gelled, but the shorter pentanoic acid was not. Simple aromatic molecules such as benzene and toluene appeared to be "too good" as solvents for CAB. The gelator was dissolved easily, with little or no heating, and remained in solution even at reduced temperatures. This behavior should be compared with that of the more polar aromatic amines and benzyl alcohol, both of which were gelled successfully. CAB did not gel the two diols examined and precipitated from poly(ethylene glycol) ($\overline{MW}$ = 600). Boiling ethanol did not dissolve CAB, and no attempt was made to superheat the mixture in a closed vessel. 1-Alkanols longer than ethanol formed very stable gels with CAB. As seen in Figure 1, T_g of 1-octanol, 63° C, is 20 °C higher than that of the *n*-alkanes. Hydrogen bonds between the 1-alkanols and CAB molecules, especially at the ether and ester oxygens, are probably responsible for the added stability.

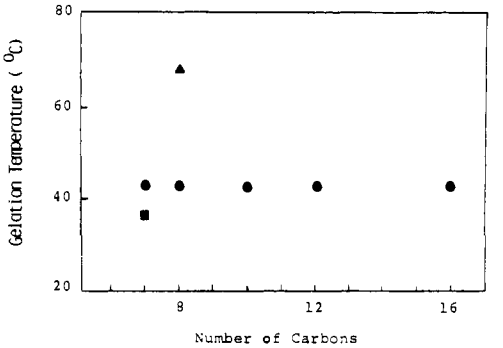

Figure 1. Gelation temperature of 0.8% (w/w) CAB/fluid gels versus the number of carbons in the fluid component. Fluid components are *n*-alkanes (●), methylcyclohexane (■), and 1-octanol (▲).

The comportment of carbonyl-substituted alkanes provides another indication that molecular structure of the fluid (and, therefore, specific fluid–gelator interactions) can be an important consideration in gel formation. None of the 2- or *sym*-alkanones employed, including 4-heptanone, provided a gel with CAB.

Table IV. Organic Fluids Tested for Gelation by CAB

organic fluid	% of CAB[a]	cooling method	phase formation[b]
1-bromopropane	1.4	*c, d, e*	N
1-bromo-3-phenylpropane	1.54	*c*	N
		d	Y
pentane	1.20	*c, d*	Y
hexane	0.80	*c*	Y
heptane	0.80, 2.7	*c*	Y
octane	0.81	*c*	Y
dodecane	0.10	*c*	N (sol)
	0.25, 0.39, 0.41, 0.81, 1.43, 1.73, 2.20, 4.1	*c*	Y
		c	Y
		c	Y
tetradecane	2.23	*c*	Y
hexadecane	0.81, 2.9	*c*	Y
heptadecane	3.00	*c*	Y
octadecane	2.70	*c*	Y
eicosane	1.57	*c*	Y
isooctane	0.81	*c*	Y
cyclohexane	1.41	*c, d*	Y
methylcyclohexane	0.80	*c*	Y
Decalin	1.56	*c, d*	Y
1-tetradecene	1.50, 4.8	*c*	Y
1-propanol	1.50	*c*	Y
1-dodecanol	1.52	*c*	Y
1-octanol	0.80	*c*	Y
1,3-propanediol	1.33, 1.09	*c, d*	N
benzyl alcohol	1.52, 1.50	*c*	Y
4-heptanol	1.53	*c*	Y
2-butene-1,4-diol	1.33	*c, d, e*	N (ppt)
3,3-dimethyl-2-butanol	1.43	*c*	N (sol)
	0.72	*d*	Y
heptanal	1.51	*c*	Y
nonanoic acid	1.61	*c, d*	Y
valeric acid	1.47	*c*	N (sol + ppt)
n-pentyl acetate	1.51	*c*	N (soln)
		d (5 °C)	Y
n-butylamine	1.50	*c*	N (sol)
		d	Y
benzylamine	1.46	*c*	N
		d	Y
N-methylbenzylamine	1.25	*c*	N (soln)
		d	Y
α-methylbenzylamine	1.49	*c*	N (soln)
		d, e	Y
benzene	1.50	*c, d, e*	N (soln)
toluene	1.33, 2.31	*c, d, e*	N (soln)
di-*n*-hexyl ketone	1.48	*c, d, e*	N (ppt)
2-octanone	1.55, 0.99	*c, d, e*	N (ppt)
2-undecanone	1.54	*c, d*	N (ppt)
4-heptanone	1.53	*c, d, e*	N (ppt)
1,2-dimethoxyethane	1.46	*c*	N (ppt)
		e	Y
1,3-pentadiene	1.46	*c*	N (soln)
		e	Y

[a] By weight. [b] Y = gel formed; N = no evidence of gel formation; sol = sol formation; ppt = precipitate; soln = isotropic-like solution. [c] Cooled to ambient temperatures in the air. [d] Cooled under cold (ca. 5 °C) running water. [e] Cooled in the freezing compartment of a refrigerator (<-10 °C).

However, heptanal formed a gel that was exceedingly stable: it persisted for several months in a closed vessel at room temperature before returning to fluid and solid. Remarkably, the strongest physical interaction between a carbonyl-containing molecule and CAB is dipolar in nature.

Functionality of the fluid molecules can control gelation by CAB, also. Although 4-heptanone could not be gelled, 4-heptanol and CAB remained as a gel for more than 1 year when kept in a sealed vessel at room temperature. We believe that this difference derives from the hydrogen-bonding interactions that are available between 4-heptanol and CAB and their lower mutual solubility.

These observations and the aforementioned necessity to retain a steroidal alkyl tail in effective gelators suggest that the ALS and fluid molecules interact at several specific locations along the structure of each. Empirically, the fluid component must be able to dissolve CAB at elevated temperatures and interact with it as

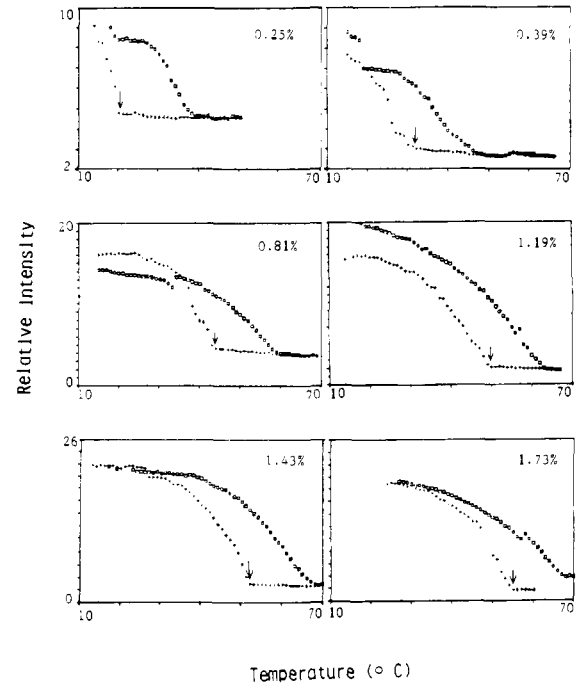

Figure 2. Relative intensities of various concentrations of CAB fluorescence at 422 nm (λ_{exc} 355 nm) in dodecane versus temperature. Heating (□) and cooling (+) cycles are shown. Arrows indicate T_g for each sample. See Figure 5 of ref 2 for a plot of T_g versus CAB concentration.

it cools and aggregates. Favorable and unfavorable interactions (i.e., solubility and insolubility) must be balanced if a gel is to form and be relatively stable. In fact, repulsive interactions may drive gelation in some ALS–fluid mixtures.[10]

The gelating abilities of other ALS were tested with fewer fluids. A protocol series (dodecane, 4-heptanol, and carbon tetrachloride) was used with ca. 1% of each. The ALS that gelled dodecane and 4-heptanol are CAB, KAB, CA-2, CAP, and CAQ. None of the ALS succeeded in gelling carbon tetrachloride. In addition to the aforementioned compounds, several others appeared to form sols with either dodecane or 1-octanol (Table III).

Gelation Process. Formation of a gel from solution requires the gelator to separate into finely dispersed colloidal particles that join together to form a continuous coherent framework throughout the fluid volume.[11] Hence, the development of a three-dimensional network by the gelator to capture small domains of isotropic fluid is critical to gel formation. The size and shape of the building blocks for the network may vary greatly between gels, but all must have an immobile framework in which the fluid is trapped. The nature of this framework and the sizes and shapes of the individual units from which the gel structures form will be discussed (vide infra).

As mentioned previously, the gelation temperature (T_g) is dependent upon the fluid component and the structure and concentration of the gelator. Figure 2 shows the change in T_g, measured by fluorescence intensity, as the concentration of CAB in dodecane is increased. In the region where [CAB] $\gtrsim$ 0.8%, T_g depends less acutely upon CAB concentration.

Below ca. 0.8% concentration and above the (unmeasured, but low) solubility limit of CAB in *n*-alkanes, sols (i.e., fracture gels) that form experience difficulties in encompassing the total fluid volume. As the CAB concentration is increased, the number of these aggregates increases until they easily occupy the total sample volume and the fluid is totally gelled. Additional CAB serves a secondary role to stabilize further the internal structure of the

(10) For studies that relate repulsive interactions and molecular ordering, see: (a) Cotter, M. A.; Martire, D. E. *J. Chem. Phys.* **1970**, *52*, 1902, 1909. (b) *Ibid.* *53*, 4500. (c) Agren, G. I.; Martire, D. E. *Ibid.* **1974**, *61*, 3959.

(11) Hermans, P. H. In *Colloid Science*; Kruyt, H. R., Ed.; Elsevier: Amsterdam, 1949; Vol. II, Chapter XII.

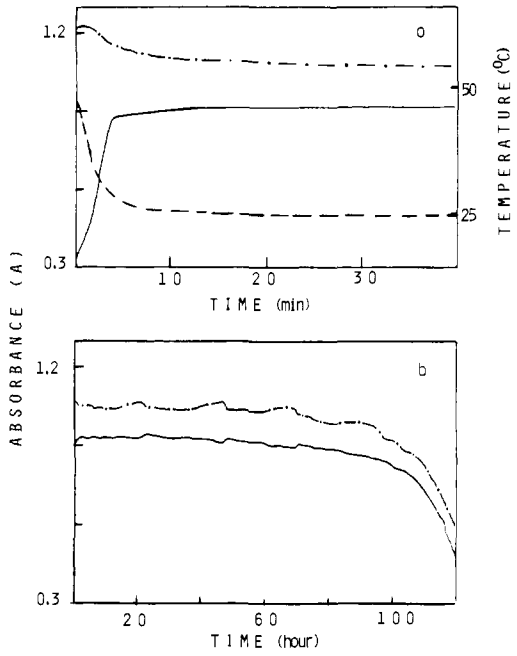

Figure 3. Gel history of a 0.49% (w/w) CAB in dodecane mixture via UV absorption changes: (a) the temperature is not constant with time (---); (b) T = 25 °C. Absorbances are at 390 nm (-·-) and at 396 nm (—).

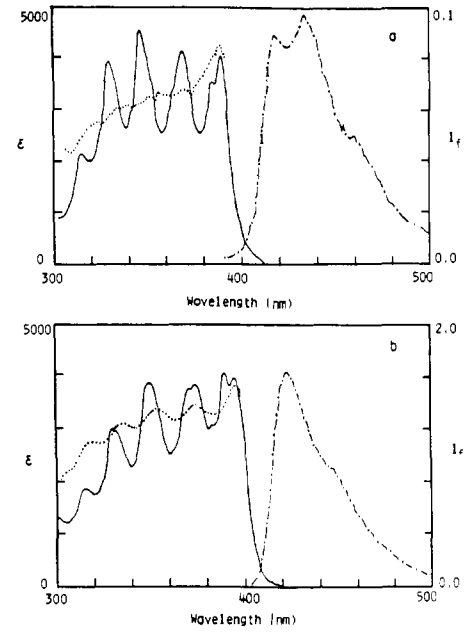

Figure 4. Molar extinction coefficients (ϵ) for absorption (—) and air-saturated emission spectra (-·-) of 0.72% (w/w) CAB in dodecane. Fluorescence intensities in (a) (T = 67 °C) and (b) (T = 25 °C) are shown to observed scale. For emission spectra, λ_{exc} = 346 nm. For excitation spectra (···), λ_{emiss} = 433 nm (a) and 422 nm (b).

fracture gels. Thus, T_g increases only slightly when CAB is added above the critical gelling concentration.

Once formed, the metastable gels revert to solid CAB and separated fluids at rates that (in conjunction with T_g) provide a qualitative measure of gel stability. For instance, the time history of a 0.49% CAB/dodecane gel was followed (Figure 3) by monitoring its absorption intensity at 390 or 370 nm (monomeric CAB) and at 396 or 376 nm (aggregated CAB). Gelation is accompanied by a pronounced increase in absorptions at 396 and 376 nm. As shown by Chandross et al., the 396- and 376-nm bands can be ascribed to excitation dipole coupling between stacked anthracenyl groups.[12] After evolution of the gel (ca. 5 min), it remains relatively stable at 25 °C for ca. 90 h. The bumps on the 390-nm curve are induced by small temperature increases and are consistent with a dynamic equilibration between monomeric and aggregated CAB, even within the gel phase. Finally, phase separation (loss of gel) beyond ca. 90 h leads to decreased absorption as CAB crystallizes and is either removed from or opaque to the ultraviolet light beam.

Although we have not followed the total life course of other ALS gels comprised of other gelators and/or fluid components, their outward appearances allow us to conclude that they experience similar qualitative changes. The duration of their stable period and the velocity of the phase separation obviously change with the gelator and the nature of its interaction with the fluid component.

Structures of CAB Gels. From Electronic Spectra. Gel formation can be followed from changes that occur in either the absorption or (more conveniently) the emission spectra of the anthryloxy portion of CAB. Up to order of magnitude increases in the fluorescence intensity and large changes in the spectral shape were observed when a warm solution of CAB was cooled and formed a gel (Figure 4). With dodecane as the fluid component, gelled CAB exhibits an emission maximum at 422 nm; the "isotropic" phase[13] of the same mixture at 67 °C has maxima at 417 and 432 nm. Since room-temperature emission spectra of very dilute solutions are shaped like the 67 °C curve, the spectral changes that attend gelation must be related to the aggregation of CAB molecules. The aggregation did not lead to an emission band ascribable to an anthracenyl excimer.[14]

The strong increase in gel fluorescence intensity can be attributed primarily to Tyndall scattering,[15a] similar to effects observed previously in liquid-crystalline media.[15b,c] However, colloidal dispersions of anthracene in water do not exhibit enhanced emission intensities.[16] Dynamic fluorescence decay curves, obtained with the time-correlated photon-counting technique,[17] were much more complex in the gel phase than in the isotropic phase. The anthracenyl groups of a 0.8% CAB in hexadecane gel at 23 °C exist in several environments since the decay profile could not be fit acceptably to a monoexponential or biexponential fit. The decay curve from the isotropic phase (69 °C) of the same mixture could be fit satisfactorily (χ^2 = 1.2) to decay constants of 8 and 13 ns. A 0.8% CAB in toluene sample that formed no gel gave simpler decay curves at 23 and 69 °C that could be fit almost completely to a single decay constant of 9 ns. When the CAB concentration was doubled, decay curves from the toluene solution at both 23 and 69 °C became multiexponential functions. We attribute the isotropic phase behavior of the 0.8% CAB/hexadecane and 1.6% CAB/toluene samples to the presence of both monomeric and aggregated CAB that probably equilibrate the way micelles and individual surfactant molecules do above the critical micellar concentration.[18] In the gel phase, nearly all of the CAB molecules above the solubility limit are in very large aggregates that are photophysically indistinguishable.

Anthracenyl absorption spectra from CAB–hexadecane solutions (Figure 4) provide further evidence for CAB aggregation

(12) (a) Chandross, E. A.; Ferguson, J.; McRae, E. G. *J. Chem. Phys.* **1966**, *45*, 3546. (b) Chandross, E. A.; Ferguson, J. *Ibid.* **1966**, *45*, 3554. (c) Ferguson, J.; Mau, A. W. H.; Morris, J. M. *Aust. J. Chem.* **1973**, *26*, 91, 103.

(13) The so-called "isotropic phase" consists of dispersed and small aggregates of CAB.

(14) (a) Cowan D. O.; Drisko, R. L. *Elements of Organic Photochemistry*; Plenum Press: New York, 1976. (b) Bouas-Laurent, H.; Castellan, A.; Desvergne, J. *Pure Appl. Chem.* **1980**, *52*, 2633. (c) Berlman, I. B. *Handbook of Fluorescence Spectra of Aromatic Molecules*, 2nd ed.; Academic Press: New York, 1971.

(15) (a) Rabek, J. F. *Experimental Methods in Polymer Chemistry*; Wiley: New York, 1980; p 187. (b) Novak, T. J.; Mackay, R. A.; Poziomek, E. J. *Mol. Cryst. Liq. Cryst.* **1973**, *20*, 231. (c) Anderson, V. C.; Craig, B. B.; Weiss, R. G. *J. Am. Chem. Soc.* **1981**, *103*, 7169.

(16) Weinberger, R.; Cline Love, L. J. *Spectrochim. Acta, Part A* **1984**, *40A*, 49.

(17) (a) Anderson, V. C. Ph.D. Thesis, Georgetown University, Washington, D.C., 1982. (b) Anderson, V. C.; Craig, B. B.; Weiss, R. G. *J. Am. Chem. Soc.* **1982**, *104*, 2972.

(18) (a) Philippoff, W. *Discuss. Faraday Soc.* **1951**, *11*, 96, 147. (b) Tanford, C. *The Hydrophobic Effect*, 2nd ed.; Wiley: New York, 1980.

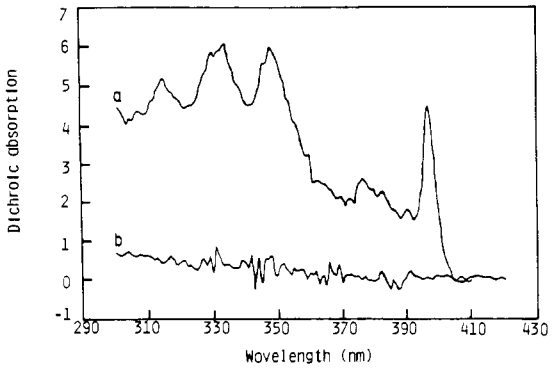

Figure 5. Circular dichroism spectra of 0.72% (w/w) CAB in dodecane in the gel (a, T = 18 °C) and isotropic (b, T = 63 °C) phases.

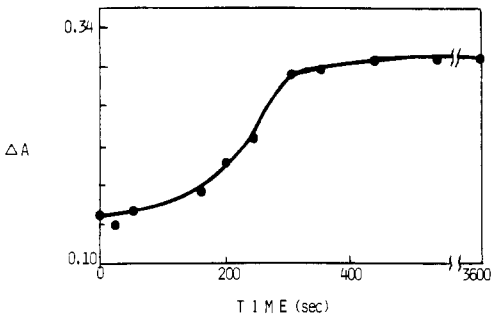

Figure 6. Variation of CD differential absorption (365 nm) during gelation of 0.72% (w/w) CAB in dodecane. The initial temperature (120 °C) cooled to the equilibrium temperature (25 °C) during the first 1800 s.

in the gel. In the isotropic phase, the 0–0 and 0–1 bands of the short-axis polarized ^1L_a absorption[19] appear at 390 and 370 nm, respectively; the two new bands at 396 and 376 nm in the gel phase, when combined with the lack of change in the long-axis polarized ^1B_b transition ($\lambda_{max} \sim 258$ nm) upon gellation, signify that neighboring anthracenyl groups are partially overlapping (stacked) but nonparallel.[12] This was further evidenced by the absence of the new bands in the absorption spectra of 0.81% CAB in a 70/30 (w/w) cholesteryl nonanoate/cholesteryl chloride mixture at 40 °C (cholesteric liquid-crystalline phase) and at ≥80 °C (isotropic phase). The cholesteric liquid-crystalline phase provides order to but not proximity between CAB molecules.

Circular dichroism (CD) spectra of the anthracenyl groups have helped to define more distinctly the nature of the aggregation among CAB molecules in the gels. The gel spectrum in Figure 5 is reminiscent of the liquid-crystal induced CD (LCICD) pioneered by Saeva.[20] LCICD is an extrinsic CD observed in liquid crystals as a consequence of the chiral array of aggregated molecules. In the gels, the appearance of a strong CD spectrum, one that includes prominently the transition dipole coupling bands at 396 and 376 nm, is strong evidence that the CAB molecules are helically stacked. The virtual absence of CD intensity from the isotropic phase of the same sample shows that the anthracenyl group of an individual, disordered CAB molecule does not experience intramolecularly the chirality of the cholesteryl group to which it is linked. In fact, the large differences in CD intensities for isotropic and gelled CAB can be used like fluorescence to follow the gelation process (Figure 6).

From X-ray Diffraction and NMR Spectra. No information concerning the structure of the gelator network could be gleaned from X-ray diffraction of gels consisting of 2% or 4% CAB in dodecane at room temperature. Only a broad hump, centered near a Bragg distance of 5–6 Å ($2\theta \simeq 9°$) could be detected from both gels. A neat sample of dodecane gave a hump whose shape, intensity, and position were indistinguishable from those of the gels. Thus, the fluid component masks diffraction from the CAB aggregates in the region scanned. The shape of the diffraction further indicates that most, if not all, of the hydrocarbon fluid is not ordered by the gelator network.

Further evidence for the isotropic nature of the fluid component in the CAB gel was obtained from 300-MHz proton ^1H NMR spectra. The dodecane signals from a 0.8% CAB/dodecane gel were indistinguishable in chemical shift and line width from those of neat dodecane. However, subtle changes in the aromatic signals from 0.8% CAB in dodecane-d_{26} were discerned as the sample passed from the isotropic to gel phase. Most of these signals became sharper in the gel phase, indicative of a reduction in the number of CAB environments. Additionally, an isotropic phase doublet near δ 7.05 moved slightly downfield and a doublet of doublets at δ 7.75 became a simple doublet. These changes occur abruptly at 44 °C, very near the T_g measured by fluorescence.

Photodimer Distributions of CAB in Gels. Previously,[3] we detailed the photochemistry of CAB in various phases, including the neat cholesteric liquid crystal. Arguments were presented to substantiate the correlation between the ratio of head-to-head (HH-4) and head-to-tail (HT-4) photodimers (eq 1) and the

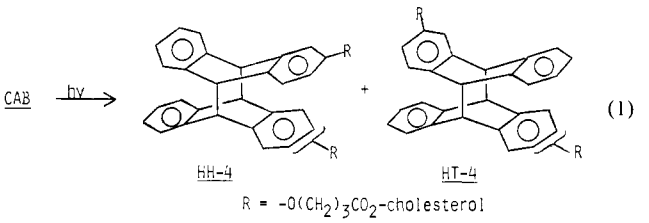

(1)

packing arrangement of CAB molecules prior to irradiation. In essence, the short singlet lifetime of CAB and its limited mobility in the cholesteric phase preclude significant deviations in the packing arrangement between the moments of anthracenyl excitation and dimerization. Thus, eq 2 (in which χ_{HH} and Φ_{HH} are the mole fraction of head-to-head CAB ground-state pairs and the quantum efficiency for dimerization from them, and Φ_{HT} is the quantum efficiency for dimerization from head-to-tail CAB ground-state pairs) is approximately correct.

$$\frac{[\text{HH-4}]}{[\text{HT-4}]} = \frac{\chi_{HH}\Phi_{HH}}{(1 - \chi_{HH})\Phi_{HT}} \qquad (2)$$

However, if a third CAB environment exists, one from which both HH-4 and HT-4 are produced, a much more complicated expression than eq 2 must be employed. The presence of some isotropic CAB (the solubility limit) and the relative sharpness of the NMR signals from CAB both argue against a simple application of eq 2 in the gel phase.

When irradiated at room temperature to ≤20% conversion, CAB–dodecane gels and CAB–toluene isotropic solutions produced 4 ratios that differ only slightly. The photodimer ratio from the neat cholesteric phase at 184 °C and that of the gel at room temperature are also quite similar (Table V). Thus, although packing considerations and the previously mentioned analyses are most consistent with the bulk of the CAB molecules in the gel phase being ordered on average in a head-to-tail fashion, the photodimer ratio does not reflect it.

From Microscopy. The CAB network of gels with 1-octanol and dodecane were revealed by a series of optical and electron microscope studies.

When viewed through crossed polarizers at 100× and cooled to their gelation temperature, hot CAB–dodecane solutions between cover glasses initially formed a faint focal conic texture. Maltese crosses are reminiscent of a liquid-crystalline pattern.[21]

(19) (a) Mason, S. F.; Peacock, R. D. *Chem. Phys. Lett.* **1973**, *21*, 406. (b) Platt, J. R. *J. Chem. Phys.* **1949**, *17*, 484.
(20) Saeva, F. D.; Wysocki, J. J. *J. Am. Chem. Soc.* **1971**, *93*, 5928.
(21) Demus, D.; Richter, L. *Textures of Liquid Crystals*; Verlag Chemie: Weinheim, 1978.

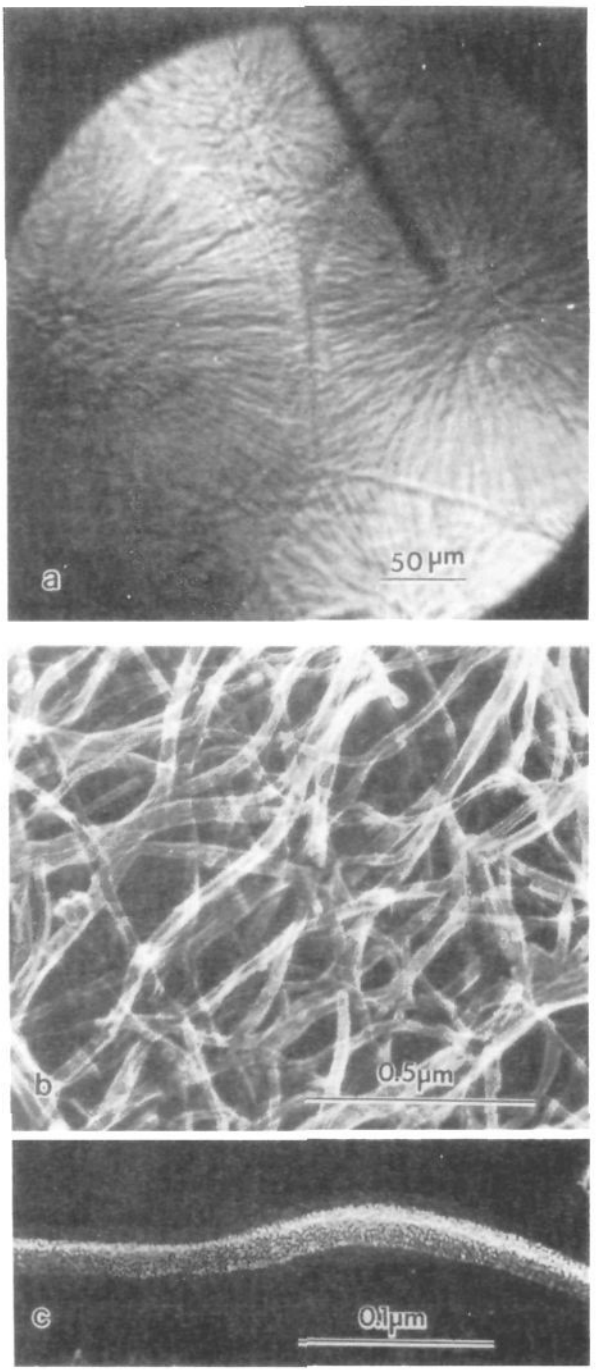

Figure 7. Optical and freeze-fracture electron micrographs of CAB/dodecane gels. (a) Optical micrograph of a 2.2% (w/w) CAB sample at room temperature; viewed through crossed polarizers. (b and c) Electron micrographs of a 2.0% (w/w) CAB sample; etched at −60 °C and 10^{-7} Torr for 1 h.

In thin samples like these, the optical pattern is indicative of the CAB molecules being in a homeotropic cholesteric-like phase. The focal conic texture rapidly gave way to elaborate fanlike domains (Figure 7a[22]) that we attribute to the network supporting the fluid component in the gel. The approximate diameter of the domains, ~200 μm, is ca. 30 times larger than the ~6–8 μm measured for the diameters of CAB/1-octanol domains (Figure 8a). When prepared as in Figure 8a (i.e., in bulk with an aliquot sandwiched between cover slips), domains of a 2% CAB in dodecane gel

(22) The correct magnification for Figure 3 in ref 2 should be 230×. The ratio between the print and negative sizes was not included in the original calculation.

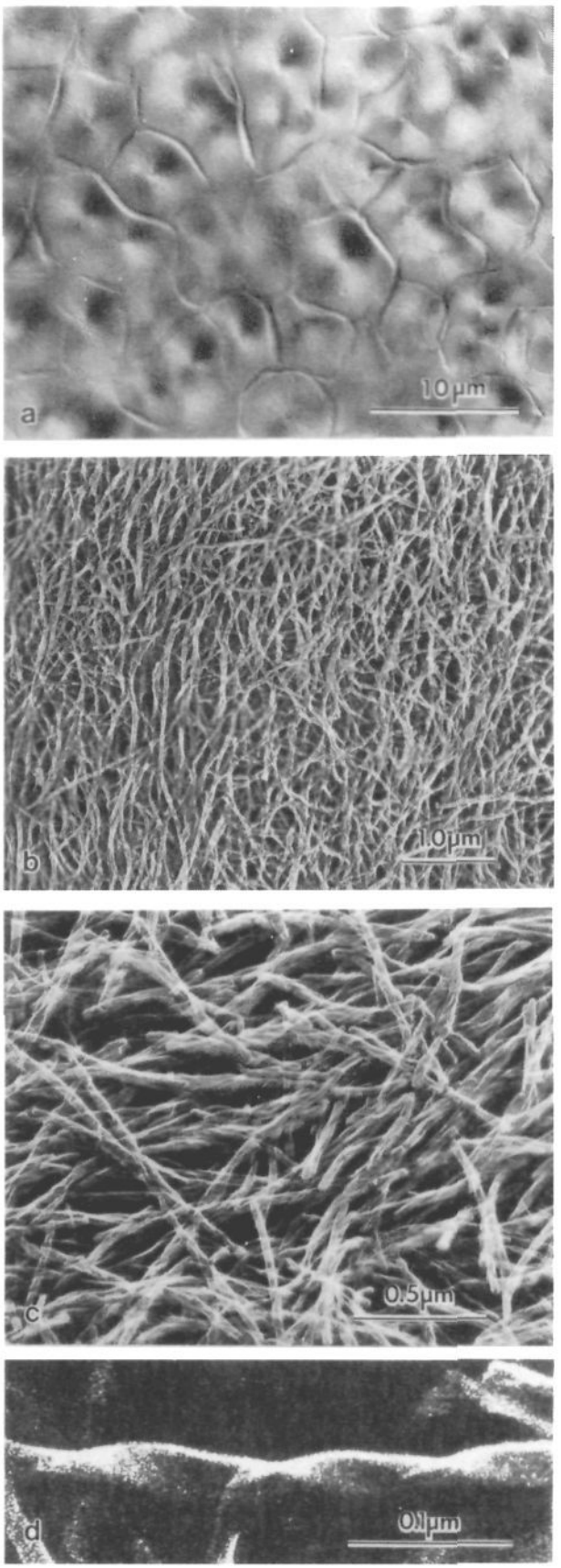

Figure 8. Optical and freeze-fracture electron micrographs of CAB/1-octanol gels. (a) Optical micrograph of a 2.0% (w/w) CAB sample. (b–d) Electron micrographs of a 1.9% (w/w) CAB sample; etched at −60 °C and 10^{-7} Torr for 1 h.

Table V. Distribution of Photodimers from CAB in Solid, Isotropic, Liquid-Crystalline, and Gel Phases

sample	phase	temp,[a] °C	**4** dimers,[c] % HT/A	HT/S	HH	conversion, %
1.12% CAB/dodecane	gel	26.0	29	19	53	<20
1.47% CAB/dodecane	gel	25.5	28	19	53	<20
1.47% CAB/toluene	isotropic	25.5	37	17	46	<20
CAB[b]	liquid-crystalline	184.4	33	12	56	
CAB[b]	liquid-crystalline	183.5	33	13	55	
CAB[b]	liquid-crystalline	178.0	34	12	54	
CAB[b]	isotropic	204.4	31	20	50	
CAB[b]	isotropic	206.7	36	17	47	
CAB[b]	solid	25.0				0

[a] ±0.2 °C. [b] Reference 3. [c] A and S refer to anti and syn configurations of HT dimers.

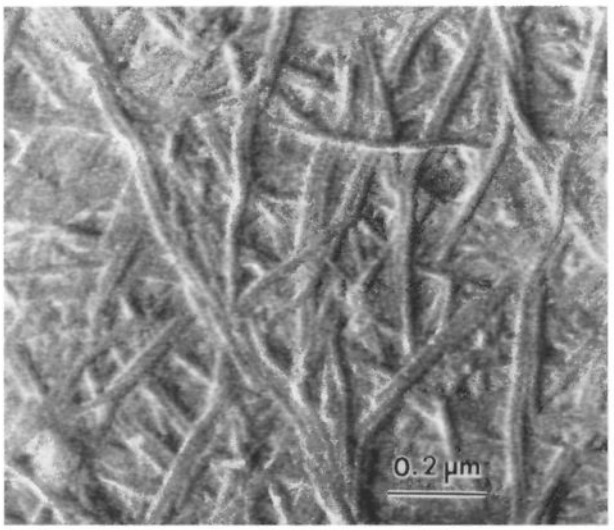

Figure 9. Freeze-fracture electron micrograph of a 1.85% (w/w) CAB in hexadecane gel; etched at −40 °C and 10^{-7} Torr for 1 h.

remained much larger than those from CAB/1-octanol gels. Although domain size may also vary with gelator concentration, a comparison of the two gels reveals the similarity between the shapes of their domains: both appear to be three-dimensional and interlocking and to consist of fibrous bundles that emanate from central points. Electron micrographs in Figures 7b and 8b,c show that the fibers of the bundles intertwine to immobilize the isotropic fluid, probably via surface tension. The morphology of a CAB/hexadecane gel (Figure 9) is very similar, as expected, to the CAB/dodecane gel.

The average width and thickness of the ribbonlike fibers of CAB/dodecane and CAB/1-octanol gels (20 random determinations) were measured from more detailed pictures such as those in Figures 7c and 8d. No measurements were taken from Figure 9 since the gel sample was etched poorly and the fibers appear to have collapsed somewhat. The dimensions of the rectangular dodecane and 1-octanol supported fibers were 20.9 (±1.5) nm × 10.4 (±0.8) nm and 26.3 (±2.1) nm × 8.2 (±1.3) nm, respectively. Neither fiber gave evidence of greater definition (i.e., multiples of smaller bundles or ordered striations). Although the majority of twists from the 1-octanol gel were left-handed, some were right-handed; Figure 8d shows both types and their average pitch is 119 (±14) nm.

Perhaps as a consequence of the weakness of the attractive forces responsible for their stability and chirality, the fibers are flexible (end fibers move in the microscope field of view) and capable of being unraveled. Fibers with an appearance remarkably similar to those in Figure 8d but whose dimensions are 2–3 times larger have been made by Pfannemuller and Welte[23] from aqueous gels of *N*-octanoyl-*N'*-gluconoylethylenediamine. Fibers from gels of steroid **2**/cyclohexane are striated (indicative of a substructure[24]) and have an average diameter of 9.1 nm.[7a] The dimensions of these and fibers from several other hydrogen-bonded gelators[25] are consistent with the CAB fibers being a wound composite of molecular threads.[26] The previously discussed electronic studies on our gels and the dimensions of their fibers (the smallest of which would require several fully extended gelator molecules to be placed end-to-end) indicate that the structures in Figures 7c and 8d are the result of several molecular threads being wrapped together, also.

At the present time, we have not determined why CAB gels with 1-octanol form twisted fibers while those with the *n*-alkanes do not. A reasonable hypothesis is that the difference is related to the way in which the CAB and fluid associate: 1-octanol can donate hydrogen bonds to specific parts of CAB while the dodecane molecules should be less specific in their interactions. The LCICD experiments performed with CAB/dodecane gels require that individual threads have CAB molecules stacked helically upon each other. In spite of this, the chiral packing is not evidenced in the more macroscopic fibers.

Conclusions

A wide variety of analytical and spectroscopic tools have been employed to characterize the macroscopic and microscopic properties of gels from ALS, a new family of thermally reversible gelators, and organic fluids. The stability of the gels depends upon the concentration of gelator, its structure, and the nature of the fluid component. While some gels can be maintained for several months, others revert to a two-phase solid/liquid mixture in several minutes.

The gelator network consists of domains of fibrous bundles that immobilize the fluid component probably by surface tension. Each fiber is several gelator molecular lengths in its smallest dimension. This observation, when combined with optical spectroscopic studies that indicate a twisted overlapping arrangement for the anthracenyl groups of the stacked gelator molecules, leads us to conjecture that each fiber consists of several molecular threads. The subtle changes that attend the CAB gelator structure with 1-octanol and dodecane as the fluid components may also occur when one fluid component is combined with different ALS gelators.[27]

The characteristics of the effective gelators synthesized here suggest that many other molecules, some with structures totally unrelated to the ALS, may gel organic fluids, also. Since only relatively weak dipolar and van der Waals forces are necessary to hold the gelator network in place, judicious molecular engineering may provide ALS gels with even greater stability than those described here.

(23) Pfannemuller, B.; Welte, W. *Chem. Phys. Lipids* **1985**, *37*, 227.

(24) See for instance: Tachibana, T.; Kayama, K.; Takeno, H. *Bull. Chem. Soc. Jpn.* **1972**, *45*, 415.

(25) (a) Tachibana, T.; Kamabara, H. *J. Am. Chem. Soc.* **1965**, *87*, 3015. (b) Hidaka, H.; Murata, M.; Onai, T. *J. Chem. Soc., Chem. Commun.* **1984**, 562. (c) Newkome, G. R.; Baker, G. R.; Saunders, M. J.; Russo, P. S.; Gupta, V. K.; Yao, Z.-q.; Miller, J. E.; Bouillion, K. *Ibid.* **1986**, 752. (d) Fuhrhop, J.-H.; Schnieder, P.; Rosenberg, J.; Boekema, E. *J. Am. Chem. Soc.* **1987**, *109*, 3387.

(26) A model for thread and fiber formation in gels comprised of small gelator molecules has been formulated: Lin, Y.-c. Ph.D. Thesis, Georgetown University, Washington, D.C., 1987.

(27) Kunitake, T.; Okahata, Y.; Shimomura, M.; Yasunami, S.-i.; Takarabe, K. *J. Am. Chem. Soc.* **1981**, *103*, 5401.

Experimental Section

Instrumentation. Circular dichroism spectra were obtained with a JASCO ORD/UV 5 with a CD attachment. Samples in a cylindrical quartz cuvette (0.5-mm path length) or 0.4-mm path-length Kimax capillaries were thermostated to ±0.5 °C. Infrared spectra were recorded and calibrated on a Perkin-Elmer PE-457 grating spectrophotometer using KBr pellets for solid samples and films between NaCl plates for liquid samples. NMR spectra were obtained on a 90 MHz Fourier transform Bruker HFX/WH-90 or a Bruker AM-300 WB 300-MHz spectrometer.

Optical microscopy was viewed through a Kofler hot-stage microscope (usually at 100×) with a plane polarizer above and below the sample stage (from which melting points and transition temperatures were measured) or a Zeiss Axiomat microscope (usually at 1000×) in the differential interference contrast mode and equipped with an internally corrected 100× 1.3 NA planapochromatic objective and a 1.4 NA condenser.

Fluorescence decay curves were obtained with an Ortec single-photon counter equipped with a Nucleus PCA multichannel analyzer interfaced to an IBM microcomputer.[17] High-performance liquid chromatography (HPLC) was performed on a Waters Associates liquid chromatograph equipped with a Model 440 constant-wavelength (254 nm) absorbance detector and a Rad-Pak B silica column (10 × 0.8 cm; 10-μm particle) in a radial compression module. Elemental analyses were performed by E+R Microanalysis Laboratory, Corona, NY.

Freeze Etching Electron Microscopy. Aliquots of each gel, ca. 1 mm^3, were placed on a fast-freezing specimen holder[28] and frozen either by immersion in liquid nitrogen or by contact with a liquid helium cooled copper block.[28] Frozen specimens were transferred to a Balzers BAF 301 freeze-etching unit, fractured at −150 °C, and allowed to etch for 1 h at 10^{-7} Torr and either −60 °C (CAB/1-octanol and CAB/dodecane gels) or −40 °C (CAB/hexadecane gel). Replicas were made by rotary shadowing the surface of the specimen from a 20° angle with a platinum/carbon electron beam gun and reinforced with a 100–200-Å carbon film. Replicas were washed in chloroform, mounted on grids, and examined in a JEOL 100 CX electron microscope. Electron micrographs are presented in the form of negative prints in which platinum deposits appear white.

Fluids and ALS Syntheses. All fluids were available commercially as reagent grade or better unless stated otherwise. The syntheses of CAB, several ALS that did not gel selected fluids, and several of the intermediates leading to ALS have been described in detail elsewhere.[3,26]

Cholesteryl Anthraquinone-2-carboxylate (CA-Q). A mixture of 0.30 g (1.2 mmol) of anthraquinone-2-carboxylic acid and 0.9 mL of oxalyl chloride in 25 mL of dry benzene was stirred and heated (bath temperature ca. 40–50 °C) in a dry atmosphere for 1 h. Benzene and excess oxalyl chloride were removed by vacuum distillation. The crude acid chloride, a yellow solid residue, was washed rapidly with benzene and was stirred for 16 h at ambient temperature under a dry atmosphere with 0.46 g of cholesterol in 20 mL of benzene and 2 drops of pyridine. A yellow solid, obtained after benzene was removed on a rotary evaporator, was recrystallized twice from chloroform/methanol to yield 0.55 g (75%), mp 229 °C (enantiotropic liquid-crystalline phase: 170–229 °C). ^1H NMR ($CDCl_3$/TMS) δ 8.87, 8.23–8.40, 7.72–7.80 (7 H, m, Ar*H*), 5.4 (1 H, d, alkenyl), 4.8–5.0 (1 H, m, oxycyclohexyl), 0.6–2.6 (43 H, m, cholesteryl). IR (KBr) 2800–3050, 1680 (quinone carbonyl), 1730 (ester), 1600, 1550, 1470–1480, 1385, 1330, 1290–1270, 1260–1240, 1175, 1130, 1100, 1040–1000, 940, 880, 800, 715 cm^{-1}. Elemental analysis: calcd for $C_{42}H_{52}O_4$, C 81.25, H 8.44; found, C 80.60, H 8.75.

Cholestanyl Anthraquinone-2-carboxylate (CHAQ). The acid chloride of 0.14 g (0.6 mmol) of anthraquinone-2-carboxylic acid was prepared as described above. It was stirred for 18 h at ambient temperature under nitrogen atmosphere with 0.22 g (0.6 mmol) of cholestanol in 25 mL of benzene and 4 drops of pyridine. A yellow solid, obtained after removal of benzene on a rotary evaporator, was recrystallized twice from chloroform/methanol to yield 0.23 g (62%), mp ca. 236 °C (uncorrected) (enantiotropic cholesteric liquid-crystalline phase: 190–236 °C). ^1H NMR ($CDCl_3$/TMS) δ 8.86, 8.23–8.40, 7.71–7.85 (7 H, m, Ar*H*), 5.10–4.85 (1 H, m, oxycyclohexyl), 0.60–2.66 (45 H, m, cholestanyl). IR (KBr) 2800–3050, 1680 (quinone carbonyl), 1730 (ester) cm^{-1}.

Cholesteryl Anthracene-2-carboxylate (CA-2). A mixture of 0.10 g (0.5 mmol) of anthracene-2-carboxylic acid (Pfaltz and Bauer) and 0.4 mL of oxalyl chloride in 50 mL of dry benzene was stirred and refluxed (bath temperature ca. 50–80 °C) under a dry atmosphere for 16 h. A yellow solid was obtained after removal of solvent and excess oxalyl chloride by vacuum distillation. The crude acid chloride was washed quickly with benzene and was mixed with a solution of 0.17 g of cholesterol in 20 mL of benzene containing a trace of pyridine. After 3 h of stirring and refluxing (bath temperature ca. 50–70 °C), 50 mL of distilled water was added. The mixture was extracted with chloroform (3 × 25 mL). The organic layer was washed twice with 25 mL of 10% aqueous sodium hydroxide and twice with 25 mL of distilled water. A yellow solid, obtained after evaporating the liquid on a rotary evaporator, was recrystallized twice from *tert*-amyl alcohol to yield 0.11 g (41%) of needle crystals, mp ca. 225 °C (enantiotropic cholesteric liquid-crystalline phase: 220–225 ± 5 °C). ^1H NMR ($CDCl_3$/TMS) δ 8.57 (1 H, s, Ar*H*), 8.46 (1 H, s, Ar*H*), 7.90–8.16 (3 H, m, Ar*H*), 7.40–7.62 (4 H, m, Ar*H*), 5.46 (1 H, d, alkenyl), 5.11–4.86 (1 H, m, oxycyclohexyl), 0.70–2.64 (43 H, m, cholesteryl). IR (KBr) 1710, 1270, 1235 cm^{-1}. Elemental analysis: calculated for $C_{42}H_{54}O_2$, C 85.37, H 9.21; found, C 85.15, H 9.21.

Cholesteryl 5-(2-Anthryloxy)pentanoate (CAP). A 25-mL solution of dimethylformamide and 0.70 g (3.6 mmol) of 2-hydroxyanthracene[3] were added, with stirring, to 20 mL of dimethylformamide containing ca. 0.1 g of sodium hydride. After hydrogen evolution ceased, 2 mL of ethyl 5-bromopentanoate (Aldrich) was added to the solution. After stirring for 24 h under a dry atmosphere, 50 mL of water was added to the reaction mixture. It was extracted with methylene chloride (5 × 50 mL). The combined organic layers were washed with 50 mL of 10% aqueous sodium carbonate and water (4 × 50 mL) and then dried over anhydrous magnesium sulfate. After evaporation of the solvent, the crude product was crystallized three times from 95% ethanol to yield 0.92 g (81%) of ethyl 5-(2-anthryloxy)pentanoate, mp 112–114 °C. IR (KBr) 1740 (ester), 1630, 1460, 1440, 1390–1370, 1270, 1245, 1210–1180, 1010, 885, 805, 740 cm^{-1}. ^1H NMR ($CDCl_3$/TMS) δ 8.35 (1 H, s, anthracenyl meso proton), 8.25 (1 H, s, anthracenyl meso proton), 7.8–8.0 (3 H, m, oxyanthracenyl protons), 7.4–7.6 (2 H, m, oxyanthracenyl protons), 7.15–7.35 (2 H, m, oxyanthracenyl), 4.0–4.3 (4 H, m, $MeCH_2OC{=}O$ and $ArOCH_2CH_2$–), 2.4–2.5 (2 H, t, J = 6.9 Hz, $-CH_2CH_2COO$), 1.8–2.0 (4 H, m, $ArOCH_2CH_2CH_2COO$–), 1.3 (3 H, t, J = 6.9 Hz, CH_3CH_2O–).

Ethyl 5-(2-anthryloxy)pentanoate (0.86 g, 2.7 mmol) was dissolved in 100 mL of hot 95% ethanol, and the solution was added to 10 mL of aqueous 50% NaOH. The turbid mixture was boiled to allow the ethanol to evaporate slowly. When the vapors no longer contained the smell of alcohol, ca. 500 mL of hot water were added. The resulting clear solution was acidified with dilute hydrochloric acid until a precipitate formed. The precipitate was extracted with chloroform (3 × 50 mL), and the combined extracts were evaporated (rotary evaporator) to yield a yellow solid. It was recrystallized from toluene to yield 0.60 g (75%) of 5-(2-anthryloxy)pentanoic acid as yellow needle crystals, mp 196–200 °C. IR (KBr) 3200–2550, 1700 (acid), 1635, 1600, 1470, 1445, 1420–1410, 1300–1250, 1220, 1190, 1040–1020, 895, 800, 745 cm^{-1} ^1H NMR ($CDCl_3$/TMS) δ 8.35 (1 H, s, anthracenyl meso proton), 8.25 (1 H, s, anthracenyl meso proton), 7.85–8.0 (3 H, m, oxyanthracenyl protons), 7.35–7.50 (2 H, m, oxyanthracenyl protons), 7.10–7.20 (2 H, m, oxyanthracenyl protons), 4.15 (2 H, t, J = 5.8 Hz, $ArOCH_2CH_2$), 2.5 (2 H, t, J = 6.9 Hz, $-CH_2CH_2COO$), 1.9 (4 H, m, $ArCH_2CH_2CH_2CH_2COO$), 1.4–1.75 (br, H_2O).

A mixture of 5-(2-anthryloxy)pentanoic acid (0.58 g, 2.0 mmol), 15 mL of dry benzene, and 5 mL of oxalyl chloride was stirred and heated under a dry atmosphere for 2 h. Benzene and excess oxalyl chloride were distilled under vacuum. The yellow residue was then mixed with a solution of 25 mL of benzene, 0.39 g of cholesterol, and a trace of pyridine. After ca. 16 h of stirring under a dry atmosphere at ambient temperature, the solvent was evaporated, and the residue was recrystallized three times from methanol/chloroform to yield 0.96 g (70%) of **8**, mp 136–137 °C. ^1H NMR ($CDCl_3$/TMS) δ 8.32 (1 H, s, anthracenyl proton), 8.24 (1 H, s, anthracenyl meso proton), 7.83–8.00 (3 H, m, oxyanthracenyl protons), 7.35–7.46 (2 H, m, oxyanthracenyl protons), 7.10–7.24 (2 H, m, oxyanthracenyl protons), 5.36 (1 H, s, alkenyl), 4.60–4.70 (1 H, m, oxycyclohexyl), 4.14 (2 H, t, J = 6.1 Hz, $ArOCH_2$), 2.56 (2 H, t, J = 6.9 Hz, CH_2COO), 0.67–2.4 (47 H, m, methylenes and cholesteryl protons). IR (KBr) 3000–2810, 1740 (ester), 1630, 1460, 1440, 1390–1370, 1270, 1245, 1210–1180, 1010, 885, 805, 740 cm^{-1}. Elemental analysis: calcd for $C_{46}H_{62}O_3$, C 83.34, H 9.43; found, C 83.43, H 9.66.

6-Ketocholestanyl 4-(2-anthryloxy)butanoate (KAB) was synthesized by esterification of 4-(2-anthryloxy)butanoyl chloride (from 0.094 g of 4-(2-anthryloxy)butanoic acid and 4 mL of oxalyl chloride in 50 mL of dry benzene) with 0.14 g (3.5 mmol) of 3β-hydroxy-6-cholestanone (Aldrich). The procedure was the same as that employed to synthesize CAB.[3] The crude product was recrystallized three times from methanol/chloroform to yield 0.17 g (73%), mp 201–203 °C. ^1H NMR ($CDCl_3$/TMS) δ 8.2–8.35 (2 H, m, anthracenyl meso protons), 7.80–8.00 (3 H, m, oxyanthracenyl), 7.35–7.45 (2 H, m, oxyanthracenyl protons),

(28) Heuser, J. E.; Resse, T. S.; Dennis, M. J.; Jan, Y.; Evans, L. *J. Cell. Biol.* **1979**, *81*, 275.

7.10–7.20 (2 H, m, oxyanthracenyl protons), 4.65–4.80 (1 H, m, oxycyclohexyl in 6-ketocholestanyl), 4.15 (2 H, t, J = 4.7 Hz, ArOCH_2), 2.74 (2 H, t, CH_2COO), 2.55, 2.4–2.15, 2.1–1.0, 0.91–0.84, 0.75, 0.64 (47 H, m, ketocholestanyl moiety and methylene). IR (KBr) 3000–2900, 2870, 1740–1700 (carbonyl), 1630, 1460, 1385, 1300, 1280–1240, 1210, 1190, 1050, 1020, 885, 805, 745 cm^{-1}. Elemental analysis: calcd for $C_{45}H_{59}O_4$, C 81.40, H 8.96; found, C 81.00, H 8.56.

Cholesteryl 2-(2-Anthryloxy)ethanoate (3). A solution of 25 mL of dimethylformamide and 0.70 g (3.6 mmol) of 2-hydroxyanthracene[3] was added, with stirring, to 20 mL of dimethylformamide containing ca. 0.1 g of sodium hydride. After hydrogen evolution ceased, 2 mL of ethyl 2-bromoacetate (Aldrich) was added to the solution, the mixture was stirred for 24 h under a dry atmosphere, and 50 mL of water was added to the reaction mixture. It was extracted with methylene chloride (5 × 50 mL), and the combined organic layers were washed with 50 mL of 10% aqueous sodium carbonate and water (4 × 50 mL) and then dried over anhydrous magnesium sulfate. After evaporation of the solvent, the crude ethyl 2-(2-anthryloxy)ethanoate was recrystallized three times from 95% ethanol to yield 0.78 g (78%) of crystals, mp 157–158 °C. ^{1}H NMR ($CDCl_3$/TMS) δ 8.35 (1 H, s, anthracenyl meso proton), 8.15 (1 H, s, anthracenyl meso proton), 7.9–8.0 (3 H, m, oxyanthracenyl protons), 7.4–7.6 (2 H, m, oxyanthracenyl protons), 7.15–7.35 (2 H, m, oxyanthracenyl protons), 4.8 (2 H, s, ArOCH_2COO–), 4.3–4.4 (2 H, q, J = 7.2 Hz, MeCH_2OC=O), 1.3 (3 H, t, J = 7.2 Hz, CH_3CH$_2$OC=O). IR (KBr) 3000–2840, 1770 (carbonyl), 1640, 1600, 1470, 1400–1380, 1310, 1285, 1220–1180, 1100–1070, 900, 830–800, 760, 730 cm^{-1}.

Ethyl 2-(2-anthryloxy)ethanoate (0.50 g, 1.8 mmol) was dissolved in 100 mL of hot 95% ethanol, and the solution was added to 10 mL of aqueous 50% NaOH. The turbid mixture was boiled to allow the ethanol to evaporate slowly, and water was constantly added to retain the total volume of solution. When the vapors no longer contained the smell of alcohol, ca. 500 mL of hot water was added. The resulting clear solution was acidified with dilute hydrochloric acid until a precipitate formed. The precipitate was extracted with chloroform (3 × 50 mL), and the combined extracts were evaporated (rotary evaporator) to yield 2-(2-anthryloxy)acetic acid as a yellow solid. It was recrystallized from toluene to yield 0.25 g (56%) of yellow needle crystals, mp 219–230 °C. ^{1}H NMR ($CDCl_3$/TMS) δ 8.35 (1 H, s, anthracenyl meso proton), 8.25 (1 H, s, anthracenyl meso proton), 7.85–8.0 (3 H, m, oxyanthracenyl protons), 7.35–7.55 (2 H, m, oxyanthracenyl protons), 7.15–7.35 (2 H, m, oxyanthracenyl protons), 4.85 (2 H, s, ArOCH_2COO–), 1.4–2.0 (br, H_2O). IR (KBr) 3600–3300, 3200–2600, 1740 (carbonyl), 1635, 1495, 1470, 1440, 1420, 1315, 1280, 1255, 1220, 1200, 1100–1070, 895, 865, 830–800, 745 cm^{-1}.

A mixture of 2-(2-anthryloxy)acetic acid (0.25 g, 1.0 mmol), 15 mL of dry benzene, and 6 mL of oxalyl chloride was stirred and heated under a dry atmosphere for 2 h. Benzene and excess oxalyl chloride were distilled under vacuum. The yellow residue was then mixed with a solution of 25 mL of benzene, 0.39 g of cholesterol, and a trace of pyridine. After ca. 16 h of stirring under a dry atmosphere at ambient temperature, the solvent was evaporated and the residue was recrystallized three times from methanol/chloroform to yield 0.42 g (70%) of **3**, mp 183–187 °C. ^{1}H NMR ($CDCl_3$/TMS) δ 8.36 (1 H, s, anthracenyl meso proton), 8.25 (1 H, s, anthracenyl meso proton), 7.9–8.00 (3 H, m, oxyanthracenyl protons), 7.35–7.50 (2 H, m, oxyanthracenyl protons), 7.10–7.30 (2 H, m, oxyanthracenyl protons), 5.40 (1 H, s, alkenyl), 4.70–4.90 and 4.78 (1 H, m, oxycyclohexyl and 2 H, s, ArOCH_2COO), 0.67–2.2 (43 H, m, cholesteryl protons). IR (KBr) 3000–2840, 1770 (carbonyl), 1640, 1600, 1470, 1400–1380, 1310, 1285, 1220–1180, 1100–1070, 900, 830–800, 760, 730 cm^{-1}. Elemental analysis: calcd for $C_{43}H_{56}O_3$, C 83.18, H 9.09; found, C 83.08, H 8.83.

General Test of Gelation in Organic Liquids. A weighed amount (typically, 1% by weight) of an ALS in ca. 3 mL of an organic liquid was heated in a septum-capped test tube until the solid dissolved. The solution was then (a) left to cool to ambient temperatures in the air, (b) cooled under cold running water (ca. 5 °C), (c) cooled in the freezing compartment of a refrigerator, or (d) cooled in liquid nitrogen. The upper limit of cooling time was 2 h. Gel formation was observed while cooling or immediately after the cooling process. If a cooling process other than (a) successfully caused gelation, the gel was then examined after it was warmed to ambient temperatures. Gelation was considered successful if these two criteria were met: (1) when inverted, samples did not flow perceptibly; (2) samples were somewhat transparent but appeared to exhibit a Tyndall effect.

Spectroscopic Studies on Gels. Electronic absorption spectra were recorded on a Perkin-Elmer Model 552 spectrophotometer. Typically, a hot solution of CAB in *n*-dodecane or 1-octanol was transferred to a microcylindrical quartz cuvette with 0.5-mm optical path. The cuvette was then thermostated in a homemade cylindrical holder, the temperature was measured by a thermistor directly attached to the wall of the cuvette, and the isotropic-phase UV spectrum was recorded. For the gel-phase spectra, the sample was quickly cooled to 18 °C by passing cold water through the thermostating unit. The spectra were recorded 5 min after a temperature of 18 °C was registered by the thermistor.

Emission spectra were obtained with a Spex Fluorolog spectrofluorimeter (150-W high-pressure xenon lamp) equipped with a Datamate computer. Typically, a hot solution containing a weighed amount of CAB in benzene, *n*-heptane, *n*-decane, *n*-dodecane, *n*-hexadecane, or 1-octanol was transferred to a flattened Kimax capillary (i.d. 0.4 mm, height 1 in., width 8 mm; Vitro Dynamics) that was flame-sealed under house vacuum after the solution transformed to gel. The sealed capillary was then affixed securely inside a *n*-dodecane-filled cuvette (1-cm path length, 5 mL) that was previously thermostated. Fluorescence spectra were recorded front face from 400 to 650 nm, with excitation at 346 nm unless otherwise stated. Excitation spectra were scanned from 200 to 410 nm with the emission monochromator at 422 nm (for isotropic phases) or at 433 nm (for gel phases). Both gel phase and isotropic phase spectra were recorded at a variety of temperatures. The samples were not degassed.

Transition and Gelation Temperatures of Gels. Flattened Kimax capillaries (8 mm × 0.4 mm i.d.) containing hot solutions of an ALS and fluid were cooled and flame-sealed under house vacuum. Each capillary was then affixed inside a thermostated square 1-cm cuvette (Pyrex, 1 cm, 5 mL) filled with dodecane. Transitions between phases were registered as the variation of front-face detected fluorescence intensity at 422 nm (excitation at 355 nm) when cycling the temperatures at ca. 1.5 °C/min. The states of the phases were confirmed by visual observations.

X-ray Diffraction Studies of the Gel Phase. X-ray diffraction patterns of samples in capillary tubes (1.0-mm i.d., 0.01-mm wall thickness) were recorded on a Picker diffractometer using Mo Kα (λ = 0.7107 Å) radiation. They were scanned at ca. 24 °C from 2θ = 3° to 15° with a step of 0.1°. The NRC-Canada diffractometer routine was used as controller software with receiving slit at 2.0 mm and with a 1.5-mm incident beam collimator. Scattering at each point was collected for 10 s of integrated counts. A second scan was taken after rotating the sample by 90° to ensure proper optical alignment. Diffraction from the sample below 3° was masked by the direct beam. Scanning angles from 11.5° to 31.1° (2θ) in a separate run resulted in no observed diffraction.

Acknowledgment. We thank Professor Geoffrey Jameson for his help in obtaining the X-ray diffraction data. Dr. Walter Mahler of Dupont is thanked for providing unpublished information concerning hemifluorinated alkane gelators and for several useful discussions. Support of this work to R.G.W. by the National Science Foundation (CHE 85-17632) is gratefully acknowledged.